remote sensing

MDPI

Article

Coupling Coordination Between Urban Development and Eco-Environment in Chinese Coastal Cities: A Multisource Remote Sensing-Based Assessment

Qiang Zhang [1,2], Yongde Guo [1,*], Jun Yan [2,3], Hongyin Xiang [2] and Zhiyu Yan [2]

[1] Faculty of Data Science, City University of Macau, Macau 999078, China; d23092100141@cityu.edu.mo
[2] Satellite Big Data Division, Zhuhai Aerospace Microchips Science & Technology Co., Ltd., Zhuhai 519000, China; yanjun@qust.edu.cn (J.Y.)
[3] School of Data Science, Qingdao University of Science and Technology, Qingdao 266000, China
* Correspondence: wtkuok@cityu.edu.mo

Highlights

What are the main findings?

- The EWM–MLP adaptive weighting strategy combines the transparency of EWM with the nonlinear learning capability of MLP, enabling limited data-driven optimization of EWM-derived weights and improving the temporal responsiveness of the weighting process.
- From 2014 to 2023, the CCD values of seven representative Chinese coastal cities generally increased but the evolution of UDL and EEQ was asynchronous and city-specific, indicating differentiated coordination pathways rather than a uniform transition toward high coordination.

What are the implications of the main findings?

- The integrated framework of ecologically enhanced indicators, EWM–MLP adaptive weighting, CCD measurement, and Random Forest-based variable importance analysis provides a practical approach for evaluating coastal urban sustainability using statistical data and remote sensing data.
- The heterogeneous CCD evolution suggests that coastal city governance should shift from a uniform development model to type-specific strategies, including land-use efficiency improvement for highly urbanized cities, pollution control and industrial upgrading for port–industrial cities, and ecological conservation for tourism-oriented or ecologically livable cities.

Abstract

Coastal cities are typical regions where economic growth, population agglomeration, and eco-environmental pressures are strongly coupled. Assessing the coordination between urban development and the eco-environment is therefore important for regional sustainability. This study selected seven representative coastal cities in China—Dalian, Qinhuangdao, Qingdao, Shanghai, Fuzhou, Xiamen, and Zhuhai—and integrated multisource remote sensing data with statistical yearbook data to construct a comprehensive evaluation system for urban development level (UDL) and eco-environmental quality (EEQ). An ecologically enhanced indicator system incorporating vegetation condition index (VCI), biological richness index (BRI), normalized difference vegetation index (NDVI), and dynamic habitat index (DHI) was developed. The coupling coordination degree (CCD) model was then used to evaluate urban sustainable development from 2014 to 2023. In addition, an EWM–MLP adaptive weighting strategy was applied to refine entropy-derived weights, and

Academic Editors: Hao Zhang, Ashraf Dewan and Rui Zhou

Received: 29 March 2026
Revised: 12 May 2026
Accepted: 20 May 2026
Published: 23 May 2026

Random Forest was used to identify variables associated with CCD prediction. The results show that CCD values generally increased during the study period, indicating improved coordination between urban development and the eco-environment. However, the evolutionary pathways differed markedly among cities, and UDL and EEQ changes were not fully synchronized. The EWM–MLP strategy introduced adaptive numerical refinements to CCD values while maintaining the overall stability of coordination-level classification. Random Forest analysis showed that CCD prediction was mainly associated with a limited number of high-contribution indicators. For all indicators combined, approximately 7–10 top-ranked variables were generally required to exceed 80% of the total importance, whereas the UDL and EEQ subsystems reached this threshold with fewer indicators. UDL-related variation was mainly associated with land-use structure, population agglomeration, and economic activity, whereas EEQ-related variation was related to ecological conditions, land-cover composition, and environmental pressure. The high-importance indicators exhibited clear inter-city heterogeneity, suggesting the need for differentiated governance strategies. The proposed framework provides methodological support for sustainable development assessment and differentiated governance in coastal cities.

Keywords: coastal cities; ecologically enhanced indicator; adaptive weighting; coupling coordination degree; random forest

1. Introduction

The United Nations Sustainable Development Goals emphasize the coordination among economic growth, social inclusion, and environmental protection [1]. Under rapid urbanization, Chinese cities face increasing pressures related to economic transformation, resource constraints, and eco-environmental protection [2,3]. Coastal cities, as key spatial carriers of economic growth, population agglomeration, and opening-up, are typical regions where urban development and eco-environmental pressures are strongly intertwined. Owing to intensive land development, land–sea interactions, ecological space compression, and environmental pollution risks, the coordination between urban development and the eco-environment in coastal cities is particularly complex. Therefore, assessing the coupling coordination between urban development level and eco-environmental quality is essential for identifying regional sustainability status and supporting differentiated governance strategies.

The CCD model has been widely used in studies of urban development, human–land relationships, land-use transition, and eco-environmental assessment [4–9]. Its indicator systems are generally constructed using either direct or indirect indicator-based approaches. Indirect approaches build evaluation systems by selecting and reorganizing system elements, offering flexibility and regional adaptability, whereas direct approaches rely mainly on remote sensing or ecological data products, providing spatial continuity and comparability [10–13]. However, either approach alone has limitations in coastal city assessment. Indirect indicators can reflect economic development, population agglomeration, land use, and environmental governance, but they are less effective in capturing eco-environmental spatial heterogeneity and vegetation–habitat dynamics. Direct indicators can describe spatially continuous eco-environmental variations, but they provide limited explanatory information on human activities and governance effects. Therefore, coastal city assessment requires an integrated evaluation system that combines socio-economic interpretability, ecological spatial representation, and regional adaptability.

As a representative indirect framework, the production–living–ecological space (PLES) framework has a solid theoretical basis [14–18] and has been widely applied in watersheds, arid regions, islands, and ecologically sensitive areas [19–23]. It has become an important tool for supporting land resource utilization, spatial function evolution, and regional sustainability assessment [24–27]. However, highly urbanized coastal cities affected by land–sea interactions remain insufficiently examined [28,29]. Moreover, although PLES provides a useful functional framework for organizing production, living, and ecological dimensions, it is less effective in directly representing spatially continuous ecological conditions derived from remote sensing observations.

Indicator weighting also strongly affects comprehensive evaluation results. The entropy weight method (EWM) objectively assigns indicator weights based on indicator dispersion and provides a transparent foundation for multi-indicator evaluation. However, because EWM-derived weights are primarily determined by the statistical variation in the observed data, they may be less responsive to subtle temporal changes in complex urban development and eco-environmental systems. Multilayer perceptron (MLP) models can learn nonlinear relationships among indicators and have been used in ecosystem monitoring, land-use prediction, and remote sensing classification [30–34]. Therefore, in this study, the MLP component is introduced as a supplementary adaptive refinement module based on the EWM-derived initial weights. Its role is not to replace EWM or generate a substantially different weighting structure, but to provide a limited data-driven adjustment that enhances the temporal responsiveness of the weighting process.

Accordingly, this study integrates statistical data, land-use information, and remote sensing ecological indicators to develop a dynamically adaptive evaluation framework for coastal cities. Taking seven typical coastal cities in China from 2014 to 2023 as examples, we construct a comprehensive evaluation system for UDL and EEQ and apply the CCD model to assess urban sustainable development. For EEQ construction, direct and indirect indicator-based approaches are combined by introducing VCI, BRI, NDVI, and DHI to enhance multidimensional ecological characterization. Meanwhile, MLP is used to introduce a modest adaptive adjustment to the weights derived from EWM. In addition, identifying the factors associated with CCD evolution to explain inter-city differences and support differentiated governance is necessary. A random forest (RF) model is further used as an explanatory tool to examine the relative importance of factors associated with CCD changes, forming an integrated framework of "ecologically enhanced indicators–dynamic weighting–coordination measurement–variable importance analysis". The remainder of this paper is organized as follows. Section 2 describes the study area, data sources, and methodological framework. Section 3 presents the spatiotemporal evolution of UDL, EEQ, and CCD, as well as the results of driving factor identification. Section 4 discusses the implications, methodological contributions, limitations, and policy relevance of the findings. Section 5 summarizes the main conclusions of this study.

2. Methods

2.1. Overview of the Study Area

Chinese coastal cities are distributed in a belt-like pattern along the coastline and play an important role in economic growth, population agglomeration, industrial division, and opening-up. Owing to differences in natural geographical conditions, city size, industrial structure, and eco-environmental pressure, coastal cities exhibit clear regional gradients and development disparities. As shown in Figure 1, key coastal cities form a north–south spatial distribution pattern at the national scale, and with significant differences in development indicators such as permanent population, number of industrial enterprises, and GDP.

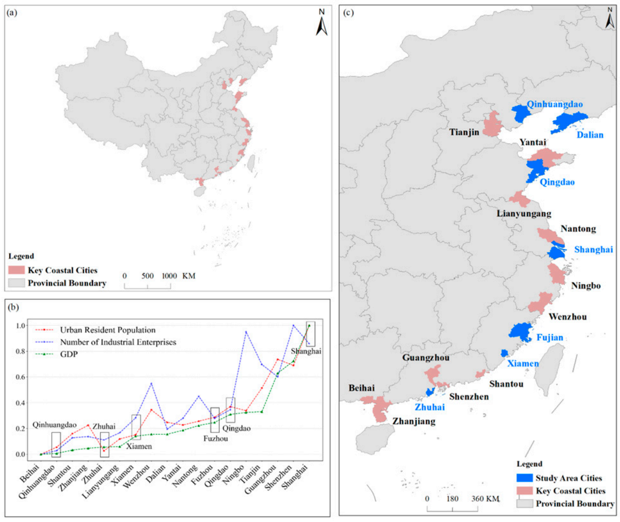

Figure 1. Map of the Study Area. (**a**) Spatial distribution of key coastal cities; (**b**) Population, Industry, and GDP of the Study Area in 2023; (**c**) Spatial distribution of the study-area cities.

Based on this spatial pattern and these development differences, this study selected representative samples by comprehensively considering regional distribution, city hierarchy, functional type, and data continuity. Priority was given to cities that cover the major north–south regions of China's coastal zone, represent different urban development characteristics, and have continuous statistical yearbook data and remote sensing observations available from 2014 to 2023. Accordingly, seven typical coastal cities—Dalian, Qinhuangdao, Qingdao, Shanghai, Fuzhou, Xiamen, and Zhuhai—were selected as study samples. Figure 1c further shows the spatial locations of these cities along China's coastal region. Among them, Dalian and Qingdao represent the port–industrial and marine-economy characteristics of northern coastal cities; Qinhuangdao represents a medium-sized port and eco-tourism city in the Bohai Rim; Shanghai represents the highly urbanized characteristics of a megacity in the Yangtze River Delta; Fuzhou and Xiamen represent a provincial capital city and an open-economy special economic zone on the southeast coast, respectively; and Zhuhai represents a bay-area node city in the Guangdong–Hong Kong–Macao Greater Bay Area that emphasizes both ecological livability and open development.

2.2. Data Sources and Indicator Selection

This study used multisource remote sensing data and statistical data from 2014 to 2023 to analyze the coupling coordination relationship in the study area. The land-use classification data are annual composite products with a spatial resolution of 30 m, generated from Landsat satellite remote sensing imagery, and were obtained from the Resource and Environment Science and Data Center of the Chinese Academy of Sciences (https://www.resdc.cn/DOI/DOI.aspx?DOIID=105 accessed on 15 December 2025). The NDVI dataset was derived from the MODIS MOD13A2 product with a spatial resolution of 1 km, while the DHI dataset was generated from the Penman–Monteith–Leuning evapotranspiration product with a spatial resolution of 500 m. Both the NDVI and DHI datasets were obtained from the National Earth System Science Data Center (https://www.geodata.cn/aboutus.html accessed on 19 December 2025). Statistical data were collected from the official statistical yearbooks of each city. The VCI and BRI were calculated according to the definitions provided in the Technical Criterion for Eco-environmental Status Evaluation [35]. The definitions are as follows:

$$VCI = Aveg \times (0.38 \times forest\ land + 0.34 \times grassland + 0.19 \times cultivated\ land + 0.07 \times construction\ land + 0.02 \times other\ land)/total\ area \quad (1)$$

$$BRI = Abio \times (0.35 \times forest\ land + 0.21 \times grassland + 0.28 \times waterarea + 0.11 \times cultivated\ land\ + 0.04 \times construction\ land + 0.01 \times other\ land) / total\ area \quad (2)$$

where *Aveg* and *Abio* represent the normalization coefficients of VCI and BRI, respectively.

Cities are characterized by intensive interactions between humans and nature, leading to high system complexity and diverse indicator selection. In this study, the economic indicators used to construct the UDL index were mainly selected with reference to previous studies [19,24], whereas the ecological indicators used to construct the EEQ index were mainly selected based on [24]. The ecological indices were inspired by the framework of [28] and further adapted to the specific characteristics of coastal cities. The results are presented in the table below. Specifically, the UDL index was designed from the perspectives of economic scale, economic activity, and economic structure and includes 10 indicators (X1–X10). The EEQ index was constructed from the perspectives of ecological structure, ecological protection, and ecological indices, and likewise includes 10 indicators (X11–X20). Among these indicators, the VCI reflects the relative vegetation condition compared with its long-term variation range and can characterize vegetation growth status and abnormal stress conditions. BRI mainly reflects bare land, construction land, and land-surface background characteristics, thereby supplementing the representation of urban expansion and surface disturbance effects on the eco-environment. Together, VCI and BRI provide ecological spatial information that is difficult to capture using only conventional socioeconomic statistics or pollution-emission indicators. In Table 1, "+" denotes a positive indicator, whereas "-" denotes a negative indicator.

Table 1. Spatial system indicators.

Element	Indicator	Code	Property
Economic Scale	GDP	X1	+
	Population	X2	+
	Population Density	X3	-
	Land Economic Density	X4	+
Economic Activity	Per Capita Fiscal Revenue	X5	+
	Fixed Asset Investment	X6	+
	Per Capita Social Retail Consumption Expenditure	X7	+
Structure of Economic	Proportion of Secondary and Tertiary Industries	X8	+
	Cultivated Land Proportion	X9	+
	Construction Land Proportion	X10	+
Structure of Ecology	Grassland Proportion	X11	+
	Forest Land Proportion	X12	+
	Bare Land Proportion	X13	+
Ecological Protection	Green Coverage Rate in Urban Built-up Areas	X14	+
	Average Urban Park Green Space per Resident	X15	+
	Urban Sewage Treatment Rate	X16	+
	Industrial Wastewater Discharge Volume	X17	-
	Sulfur Dioxide Emissions	X18	-
Ecological Indices	VCI	X19	+
	BRI	X20	+

To examine potential redundancy among indicators, multicollinearity was assessed using the variance inflation factor (VIF) based on the city–year panel dataset of the seven coastal cities from 2014 to 2023. The results showed that most indicators had acceptable or moderate VIF values, whereas relatively high VIF values were mainly observed for GDP, land economic density, and construction land proportion. This pattern is reasonable because these indicators are closely related to urban economic scale, land-use intensity, and spatial expansion. Since this study focuses on composite index construction rather than causal regression estimation, these indicators were retained to preserve the theoretical completeness and comparability of the UDL indicator system.

2.3. Research Methods

Figure 2 illustrates the technical framework of this study, which mainly consists of three components: indicator screening and model construction, adaptive weight optimization, and CCD analysis. Based on a multisource data structure, this study integrates both direct and indirect indicator-based approaches into the urban development and eco-economic evaluation framework. By incorporating VCI, BRI, NDVI, and DHI, the spatial representation of urban ecological conditions is enhanced. Meanwhile, an MLP-based adaptive weighting strategy is introduced to improve the temporal responsiveness of indicator weights. Subsequently, the CCD model is employed to analyze the coordination relationship between UDL and EEQ, and a random forest model is further used to examine the relative importance of factors associated with this coordination relationship. The key methods are described as follows.

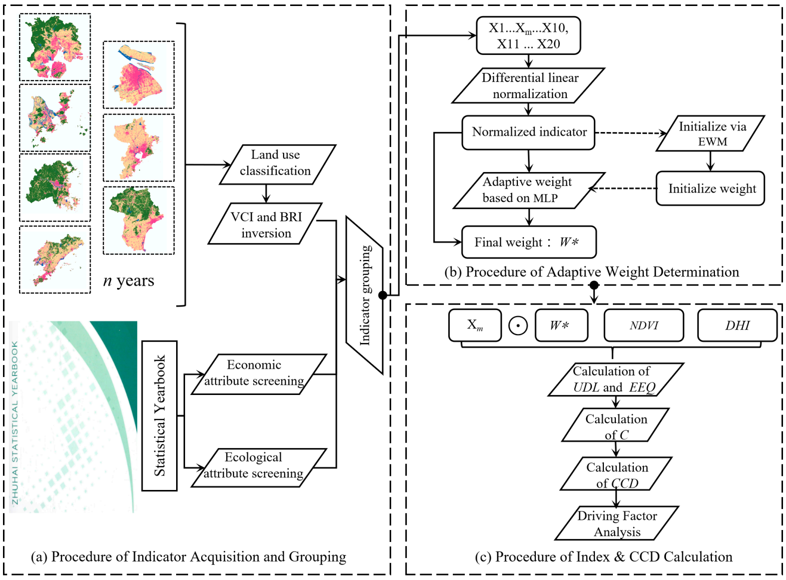

Figure 2. Technical Framework of This Article.

2.3.1. Construction of UDL and EEQ Indices

To quantitatively characterize urban development and eco-environmental conditions, two independent composite indices, UDL and EEQ, were constructed based on normalized multisource indicators:

Let

$$X^U = \left[x^U_{i,j}\right] \in \mathrm{R}^{m_U \times n} \tag{3}$$

$$X^E = \left[x^E_{k,j}\right] \in \mathrm{R}^{m_E \times n} \tag{4}$$

denote the normalized indicator matrices for the urban development and eco-environmental systems, respectively, where m_U and m_E are the numbers of indicators and n is the number of years. The element $x_{i,j}$ represents the normalized value of the corresponding indicator in year j.

For a given year j, the UDL index is defined as a weighted linear aggregation of urban development indicators:

$$UDL_j = W^{UT} X_j^U = \sum_{i=1}^{m_U} w_i^U x_{i,j}^U \tag{5}$$

where $W^U = \left[w_1^U, w_2^U, \ldots, w_{m_U}^U\right]^T$ is the weight vector of urban development indicators, satisfying $w_i^U > 0$ and $\sum_{i=1}^{m_U} w_i^U = 1$. The vector X_j^U denotes the normalized urban development indicator values in year j.

To enhance the representativeness of ecological conditions across multiple spatial and temporal scales, the EEQ index was constructed using a fusion strategy that integrates environmental factor indicators with remotely sensed ecological indices. First, an eco-environmental factor composite was calculated as follows:

$$E_j^{fac} = W^{ET} X_j^E = \sum_{k=1}^{m_E} w_k^E x_{k,j} \tag{6}$$

where $W^E = \left[w_1^E, w_2^E, \ldots, w_{m_E}^E\right]^T$ denotes the weight vector of eco-environmental indicators, and X_j^E represents the corresponding normalized indicator vector in year j. The final EEQ index was obtained by fusing the environmental factor composite with the normalized NDVI and DHI:

$$\mathrm{EEQ}_j = \lambda_1 E_j^{fac} + \lambda_2 NDVI_j + \lambda_3 DHI_j \tag{7}$$

where λ_1, λ_2, and λ_3 are the weights of the environmental-factor composite value, NDVI, and DHI, respectively, and $\lambda_1 + \lambda_2 + \lambda_3 = 1$. Equal weights are adopted in this study as a baseline fusion strategy rather than as an assumption that the three components have identical ecological importance. The environmental factor composite value, NDVI, and DHI represent complementary ecological dimensions related to environmental status, vegetation coverage, and habitat dynamics. In the absence of a generally accepted prior weighting scheme for these heterogeneous components, equal weighting provides a transparent and neutral approach for integrating them while avoiding additional subjective preference.

2.3.2. MLP-Based Adaptive Weight Adjustment

Conventional composite index construction typically assumes static indicator weights, which may be insufficient for capturing temporal variations in indicator importance under evolving urbanization and environmental conditions. To address this limitation, a machine learning-based adaptive weighting strategy was introduced to dynamically adjust indicator weights by learning inter-annual evolution patterns from historical data.

Given a normalized indicator matrix $X \in R^{m \times n}$, where X can represent either X^U or X^E, supervised learning samples are constructed using adjacent-year observations, and m denotes the numbers of indicators. For year $j = 2, \cdots, n$, the input feature vector and target output were defined as:

$$S_{j-1} = X_{j-1}, t_{j-1} = X_j - X_{j-1} \tag{8}$$

where X_j denotes the normalized indicator vector in year j. This formulation enables the model to learn how the indicator state in one year is associated with its subsequent evolution. An MLP was employed to model the nonlinear mapping between indicator states and their temporal changes:

$$\Delta \hat{X}_j = F_\theta\left(X_{j-1}\right) \tag{9}$$

where $F_\theta(\cdot)$ represents the MLP with learnable parameters θ. The network consists of two hidden layers with rectified linear unit (ReLU) activation functions, enabling it to capture nonlinear interactions among indicators. The MLP was implemented using the scikit-learn MLPRegressor with two hidden layers containing 20 and 10 neurons, ReLU activation, the default Adam optimizer, squared error loss, a maximum of 1000 iterations, and a fixed random seed of 42. The learning rate and batch size followed the default settings of MLPRegressor. The predicted variation was bounded using the tanh function, with the perturbation coefficient set to 0.14.

Then, using the most recent indicator state, the predicted variation vector is obtained as:

$$\Delta\hat{X}_n = F_\theta(X_{n-1}) \tag{10}$$

The indicator weights are then adaptively updated according to:

$$W^* = W^{(0)}\left(1+\alpha\Delta\hat{X}_n\right) \tag{11}$$

where $W^{(0)}$ is the initial weight vector derived using the entropy weight method (EWM). And $\alpha \in (0,1)$ is a learning rate controlling the adjustment magnitude. To ensure interpretability and numerical stability, the updated weights are constrained to be non-negative and normalized:

$$w_i^* \leftarrow \max(0, w_i^*),\ W^* = \frac{W^*}{\sum_{i=1}^{m} w_i^*} \tag{12}$$

The resulting adaptive weights W^* were subsequently used in Equations (5) and (6) for UDL and EEQ computation, respectively. By integrating MLP-based adaptive weighting with composite index construction, the proposed framework improves the temporal responsiveness and data-driven representation of UDL and EEQ assessments, thereby providing a basis foundation for coupling coordination analysis.

2.3.3. Calculation of the CCD

Based on the constructed UDL and EEQ indices, the interaction and coordination between urban development and the eco-environmental system were quantitatively evaluated using the coupling coordination degree model. The model is defined as follows:

$$C = \frac{2\sqrt{UDL \cdot EEQ}}{UDL + EEQ} \tag{13}$$

$$T = \beta * UDL + (1-\beta) * EEQ \tag{14}$$

$$CCD = \sqrt{C \times T} \tag{15}$$

where $C \in [0,1]$. A higher value of C indicates a stronger interaction between urban development and eco-environmental systems, whereas a lower value reflects weak coupling or potential imbalance. $\beta \in [0,1]$ is a balance coefficient that reflects the relative importance assigned to urban development and eco-environmental quality. In this study, β was set to 0.5. A larger *CCD* value indicates a higher level of coordinated and sustainable development between urban growth and eco-environmental conditions. T represents the comprehensive coordination index of the two systems. Based on commonly used classification schemes in previous studies, the coupling and coordination relationship is categorized into 10 levels, as shown in Table 2.

Table 2. Coupling coordination relationship.

Range	Level	Range	Level
(0, 0.1)	Extreme Discoordination	(0.1, 0.19)	Severe Discoordination
(0.19, 0.29)	Moderate Discoordination	(0.29, 0.39)	Mild Discoordination
(0.39, 0.49)	Borderline Discoordination	(0.49, 0.59)	Marginal Discoordination
(0.59, 0.69)	Initial Coordination	(0.69, 0.79)	Intermediate Coordination
(0.79, 0.89)	Good Coordination	(0.89, 1.00)	High-Quality Coordination

2.3.4. Variable Importance Analysis

To examine the relative importance of indicators associated with CCD variation, a supervised regression task was formulated in which the response variable was the annual CCD series and the predictors were the normalized indicator vectors. Let $X \in R^{m \times n}$ denote the indicator–year matrix and $X_j \in R^m$ the indicator vector in year j. The regression model is defined as:

$$y_j = f(X_j) + \epsilon_j \tag{16}$$

where y_j is the CCD value in year j, and $f(\cdot)$ is approximated using a random forest regressor. To preserve interpretability and align with the dual-system framework, predictors are analyzed under three settings: (i) all indicators, (ii) UDL-related indicators, and (iii) EEQ-related indicators. For the UDL-related indicators, the convolution result of the normalized urban development indicator matrix X^U and the weights is used as the input for RF-based importance analysis. For the EEQ-related indicators, the EEQ index is computed by integrating environmental factor indicators with remotely sensed indices, including NDVI and DHI. As shown in Equation (17), an equal-weight fusion strategy is adopted in the EEQ construction, with weights uniformly set to $1/3$. Under this setting, directly using individual EEQ components in driving factor analysis would lead to inconsistencies between the EEQ calculation and the explanatory framework. To ensure methodological consistency, the eco-environmental system input for driving factor analysis was redefined as follows:

$$X_{EEQ} = \begin{bmatrix} X^E \\ NDVI \\ DHI \end{bmatrix} \bigodot \frac{1}{3} \begin{bmatrix} w_1^E \\ \vdots \\ w_{m_E}^E \\ 1 \\ 1 \end{bmatrix} \tag{17}$$

X_{EEQ} is employed as the effective input for RF-based driving factor analysis of the eco-environmental subsystem. Because the annual sample size was limited, with one observation per year, a clearly defined resampling and validation strategy is essential to improve the robustness of feature-importance inference. A time-aware forward-chaining validation scheme was adopted as the primary validation strategy to preserve temporal ordering. Specifically, models are trained on earlier years and evaluated on the subsequent year in a rolling manner (e.g., train: 2014–2021, test: 2022; train: 2015–2022, test: 2023), which prevents information leakage across time and provides realistic out-of-sample assessment. To further reduce the variance of importance estimation under small-sample conditions, the forward-chaining procedure is repeated under multiple random seeds, and feature importance is summarized by the mean and standard deviation across repeats. This procedure provides a stability-aware criterion for identifying core drivers, rather than relying on a single model fit or a single split.

Within each training fold, predictors are standardized using z-score normalization, where the mean and standard deviation are estimated from the training set only and then applied to the corresponding test sample. Random forest models are trained with conservative complexity control to mitigate overfitting under the limited annual samples. Specifically, the number of trees is set to 50, the maximum tree depth is set to 2, and the analysis is repeated with 10 random seeds. Feature importance is primarily quantified using permutation importance with 10 repeats and negative mean squared error as the scoring function. Permutation importance evaluates the increase in prediction error after randomly permuting one feature while keeping the other features unchanged, and it was used here to assess the relative predictive contribution of each indicator. In addition, impurity-based importance is used only for preliminary top-K screening before permutation importance is calculated for the selected variables. Indicators that repeatedly appear among the top-ranked variables across validation folds and random repeats are interpreted as high-contribution indicators associated with CCD prediction, rather than as causal drivers.

3. Results

3.1. Analysis of MLP-Optimized Weights

To evaluate the effectiveness of the proposed MLP-based adaptive weighting method, three quantitative metrics were calculated: the mean absolute change in weights, the Spearman rank correlation coefficient, and the variance change in the weight distribution.

As summarized in Table 3, the mean absolute changes in indicator weights ranged from 0.010 to 0.019, suggesting that MLP optimization introduced noticeable but non-disruptive adjustments to the entropy-derived weights. Dalian showed the largest mean and maximum absolute changes (0.019 and 0.073, respectively), whereas Qinhuangdao showed the smallest mean change (0.010). The Spearman rank correlations ranged from 0.851 to 0.953, corresponding to rank consistency values of 85.14–95.34%. This indicates that the optimized weights generally preserved the basic entropy-based ranking while allowing partial reordering of indicator importance. This pattern is further supported by Figure 3, in which most points are distributed near the equality reference line, although city-specific deviations indicate adaptive corrections to the original entropy weights. The variance of the optimized weights increased in Zhuhai, Xiamen, Shanghai, Qingdao, and Dalian, particularly in Qingdao (+54.745%) and Shanghai (+43.655%), suggesting enhanced differentiation among indicators. In contrast, the variance decreased in Fuzhou (−14.550%) and Qinhuangdao (−11.138%), indicating a smoothing effect on the original weight distribution. Overall, the EWM–MLP strategy adaptively refines the entropy-derived weights and improves the city-specific explanatory capacity of the weighting scheme.

Table 3. Quantitative comparison between entropy weights and MLP-optimized weights.

City	Mean abs Change	Max abs Change	Spearman ρ	Rank Consistency (%)	Var (EWM)	Var (MLP)	ΔVar (%)
Zhuhai	0.015	0.045	0.881	88.120	0.002	0.002	37.203
Xiamen	0.011	0.031	0.947	94.740	0.002	0.002	9.359
Fuzhou	0.013	0.032	0.868	86.770	0.001	0.001	−14.550
Shanghai	0.014	0.035	0.871	87.070	0.001	0.001	43.655
Qingdao	0.012	0.031	0.953	95.340	0.001	0.002	54.745
Qinhuangdao	0.010	0.023	0.887	88.720	0.002	0.002	−11.138
Dalian	0.019	0.073	0.851	85.140	0.004	0.005	31.054

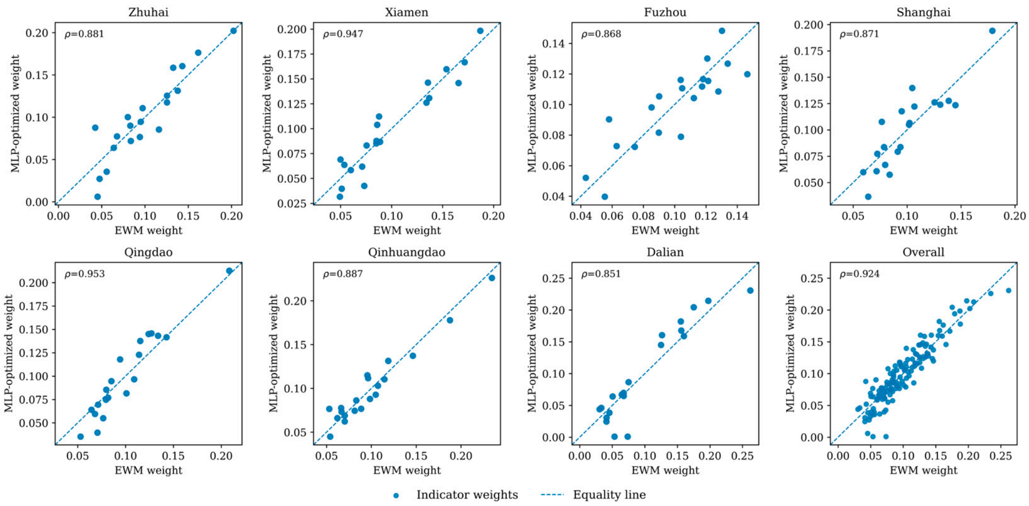

Figure 3. Consistency between entropy weights and MLP-optimized weights.

Figure 4 shows the heatmap of weight adjustments, revealing clear city- and indicator-specific heterogeneity. Positive and negative adjustments appear across different indicators and cities, indicating that the MLP module introduced adaptive corrections rather than uniform changes. For the urban development indicators, several variables related to demographic agglomeration and spatial development, such as population size (X2), population density (X3), and land economic density (X4), showed positive adjustments in some cities, including Zhuhai, Shanghai, Qingdao, and Dalian. In contrast, some land-use and consumption-related indicators, such as cultivated land proportion (X9) and per capita retail sales of consumer goods (X7), showed negative adjustments in several cities. For the eco-environmental subsystem, indicators related to ecological structure and environmental conditions, including forest land proportion (X12), per capita park green space (X15), vegetation coverage index (X19), and biological richness index (X20), exhibited different adjustment patterns across cities. These results suggest that MLP optimization captured heterogeneous indicator responses rather than applying a fixed correction pattern, further emphasizing the contributions of population agglomeration, ecological space quality, urban green-space provision, and environmental governance capacity to the UDL or EEQ subsystems.

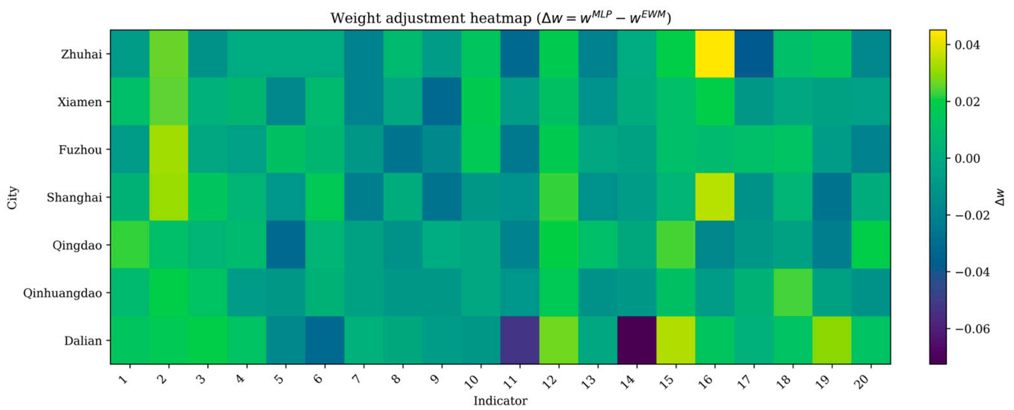

Figure 4. Heatmap of weight adjustments across cities and indicators.

The boxplots in Figure 5 further show that most Δw values were centered around zero, suggesting that the optimization process remained controlled. However, Dalian exhibited the widest adjustment range and several negative outliers, mainly associated with the strong down-weighting of several eco-environmental indicators, reflecting more evident indicator-specific reallocation. Zhuhai and Shanghai also showed relatively wide adjustment ranges, whereas Qinhuangdao presented a narrower distribution. These patterns indicate that the MLP-based correction remained bounded while allowing city-specific redistribution of indicator weights.

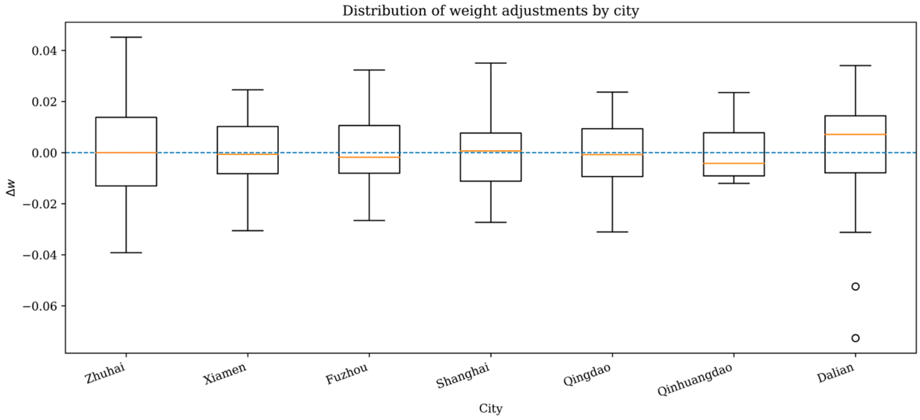

Figure 5. Distribution of weight adjustments by city.

Table 4 compares the CCD results calculated using EWM-derived and MLP-optimized weights. Overall, the MLP-based optimization produced small but observable numerical changes in the CCD values, with an overall mean absolute change of 0.008 and a maximum absolute change of 0.030. At the city level, Xiamen and Dalian showed the largest mean absolute changes, whereas Qinhuangdao showed the smallest change. However, the coordination-level classifications remained highly consistent, with an overall classification consistency of 95.7%. These results indicate that the EWM–MLP strategy improved the numerical sensitivity of CCD estimation while maintaining the robustness of the overall coordination-level classification.

Table 4. Comparison of CCD values before and after MLP-based weight optimization.

City	Mean CCD (EWM)	Mean CCD (MLP)	Mean ΔCCD	Mean |ΔCCD|	Max |ΔCCD|	Grade Consistency (%)	CCD in 2014 EWM/MLP	CCD in 2023 EWM/MLP
Zhuhai	0.68	0.68	−0.003	0.009	0.030	90.0	0.49/0.46	0.73/0.75
Xiamen	0.72	0.71	−0.004	0.012	0.030	80.0	0.56/0.53	0.80/0.81
Fuzhou	0.69	0.69	0.001	0.005	0.010	100.0	0.51/0.50	0.81/0.81
Shanghai	0.68	0.68	−0.005	0.007	0.020	100.0	0.50/0.48	0.79/0.79
Qingdao	0.69	0.69	−0.002	0.006	0.020	100.0	0.48/0.48	0.83/0.83
Qinhuangdao	0.68	0.67	−0.002	0.004	0.010	100.0	0.53/0.52	0.79/0.79
Dalian	0.63	0.63	0.002	0.012	0.030	100.0	0.66/0.65	0.76/0.79
overall	—	—	−0.002	0.008	0.030	95.7	—	—

3.2. Geographic Spatial Change Trends

Land-use patterns directly reflect the spatial allocation and utilization of urban resources and reveal urban development potential. As shown in Figure 6, the spatial distributions of different land-use types, including cultivated land, forest land, shrubland, grassland, water bodies, bare land, and construction land, as well as their increasing or decreasing trends, are illustrated. Significant differences were observed in the spatial distribution and change trends of land-use types among the seven coastal cities. Xiamen and Shanghai showed the most pronounced urban expansion, with a significant increase in construction land, indicating higher land-use intensity and faster urbanization. In contrast, Zhuhai, Fuzhou, Qinhuangdao, and Dalian retained relatively large proportions of ecological land, suggesting stronger ecological resource endowments. Qingdao, meanwhile, maintained a solid agricultural foundation, with relatively limited occupation of cultivated land during urban development. These differences indicate that each city followed a development pathway suited to its own resource conditions, providing a spatial basis for the heterogeneity of UDL–EEQ coordination.

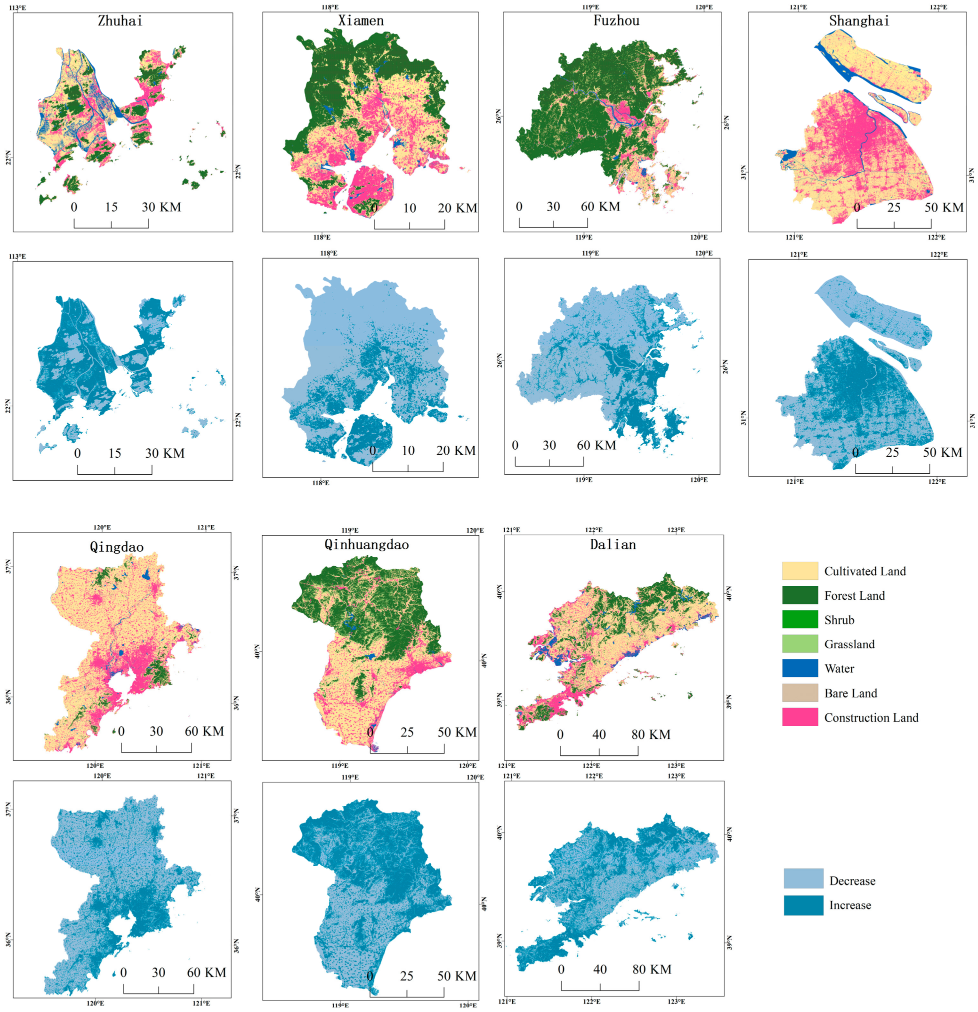

Figure 6. Land-use distribution and change trends.

Moreover, land-use evolution in the study area was not characterized by simple urban expansion, but rather by a complex process involving ecological space reorganization and agricultural land adjustment. This suggests a certain degree of competition among urban growth, ecological protection, and agricultural resource use, providing an important structural basis for understanding the coordination between urban development and eco-environmental quality.

During urban development, urban economic density reflects the intensity of land-use utilization and the level of economic development across different regions. As shown in Figure 7, the evolution of urban economic density exhibited clear stage-wise and fluctuating characteristics. Zhuhai, Xiamen, Fuzhou, and Shanghai maintained relatively stable urban development during 2015–2019, indicating a relatively favorable coordination between intensive land use and economic growth during this period. In 2020, however, the growth rate slowed or even declined, possibly due to external shocks that affected urban economic activities. Although these cities showed some recovery during 2021–2023, the pace of recovery varied across cities and remained weaker than that in the earlier period for some cities, suggesting that urban economic activities were sensitive to external disturbances. This heterogeneous recovery may be partly related to differences in industrial structure, urban hierarchy, regional coordination capacity, and policy response. For example, Shanghai's relatively faster recovery may be associated with its diversified economy, strong service sector, advanced manufacturing base, and integration within the Yangtze River Delta. In contrast, Dalian, as an old industrial and port–industrial city, may have been more constrained by its stronger dependence on traditional port–industrial activities and ongoing industrial restructuring.

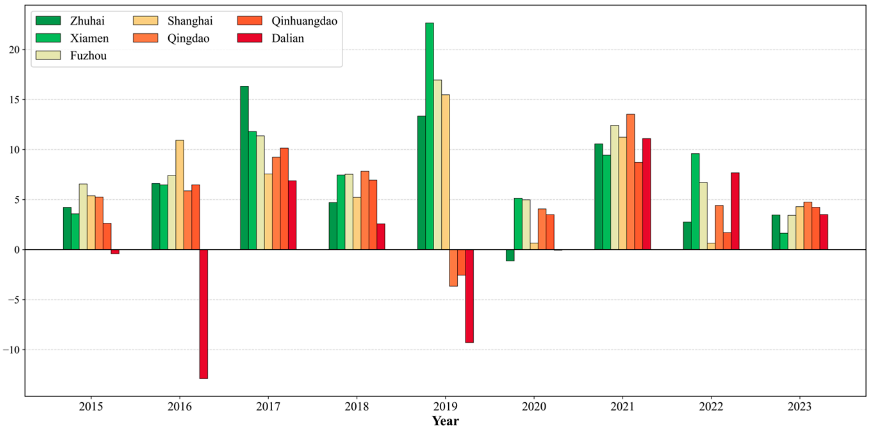

Figure 7. Growth rate of urban economic density (GDP/construction land area).

The stage-wise evolution of urban economic density suggests that the development of coastal cities was not a simple linear accumulation process, but rather a dynamic reshaping process jointly constrained by government policies, land-use restructuring, industrial transformation, and external environmental changes. Moreover, simple land expansion is no longer sufficient to meet the demands of urban development; future development will depend more on improving the quality of individual systems and optimizing their relative structure.

3.3. UDL and EEQ Evolution Characteristics

As shown in Figures 8 and 9, the spatial distributions of NDVI and DHI for each city in 2014, 2017, 2020, and 2023 are presented. The selected years balance temporal representativeness and figure readability. The two intermediate years help illustrate the evolution process without making the figure overly crowded. Overall, the city-averaged NDVI values show relatively small changes at the selected time points, suggesting that vegetation greenness remained generally stable at the aggregate city scale. However, mean NDVI is a coarse indicator and may mask spatially heterogeneous vegetation changes. Localized vegetation loss in peri-urban expansion zones may be offset by greening in urban parks, established urban areas, suburban afforestation, or ecological restoration areas. Therefore, aggregate NDVI stability should not be interpreted as evidence of the absence of vegetation disturbance.

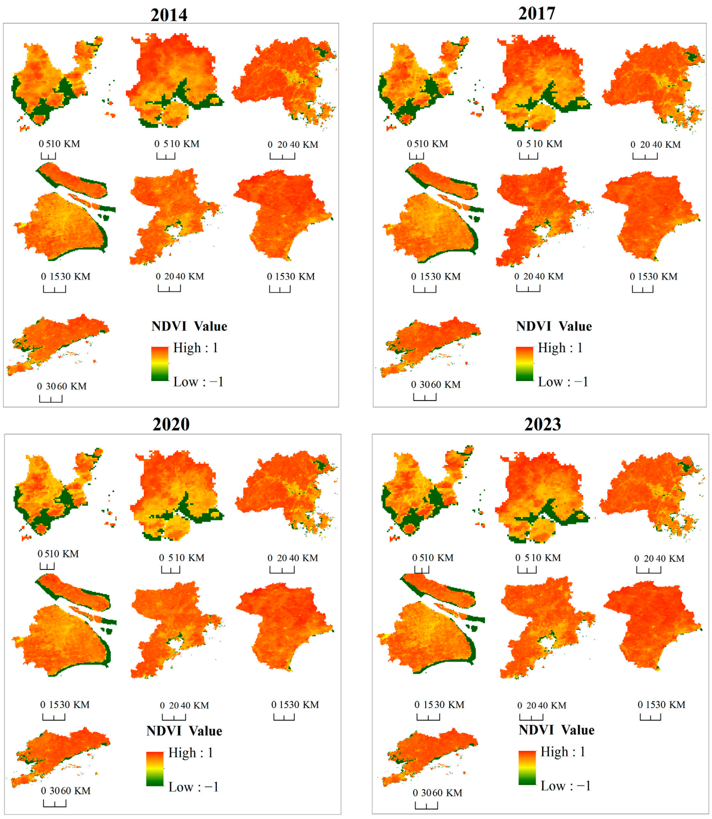

Figure 8. Spatial distribution patterns of the NDVI in the study area in 2014, 2017, 2020, and 2023.

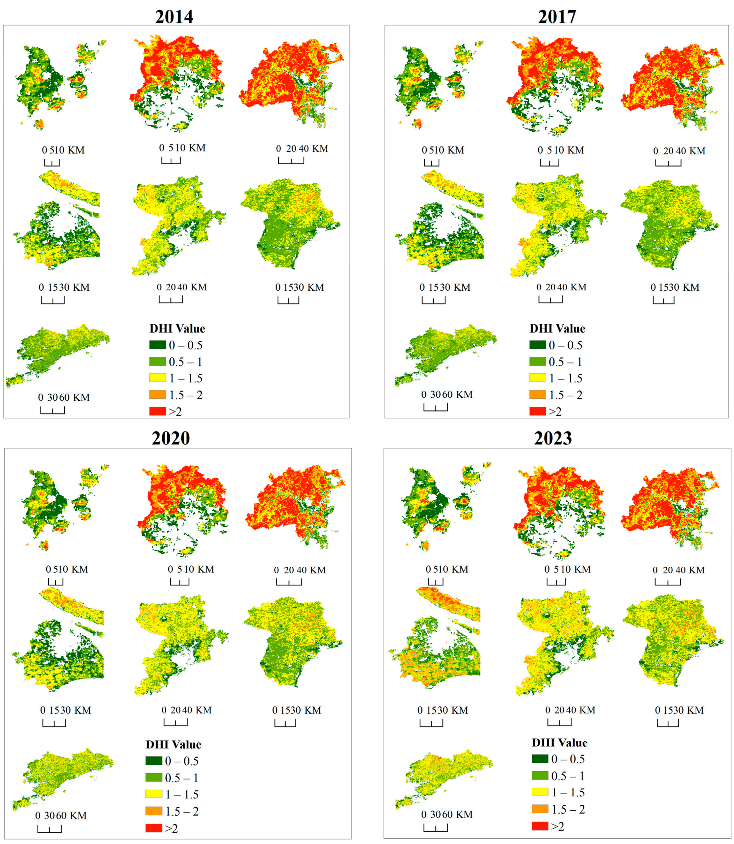

Figure 9. Spatial distribution patterns of the DHI in the study area in 2014, 2017, 2020, and 2023.

Compared with NDVI, DHI shows more pronounced intercity differences, indicating that habitat quality and ecological dynamics are not fully captured by vegetation greenness alone. Cities such as Dalian, Qinhuangdao, Qingdao, and Fuzhou exhibit relatively high DHI levels, which may be related to their ecological resources, such as mountains, water bodies, wetlands, and farmland. In contrast, more intensively developed cities, such as Zhuhai, Xiamen, and Shanghai, may face greater pressure on ecological space and rely more on artificial restoration, urban greening, and refined ecological management. Thus, NDVI and DHI provide complementary but still aggregate perspectives for urban ecological assessment: NDVI reflects vegetation greenness, whereas DHI captures habitat dynamics and ecological heterogeneity. Further spatially explicit analysis is still needed to reveal local ecological changes within cities.

Figure 10 shows the temporal evolution of UDL and EEQ in the seven coastal cities from 2014 to 2023. UDL generally increased in Zhuhai, Xiamen, Fuzhou, Shanghai, Qingdao, and Qinhuangdao, indicating continuous improvement in urban development associated with economic growth, population concentration, land-use intensity, and industrial activity. In contrast, EEQ exhibited more complex and fluctuating trajectories. Zhuhai and Shanghai showed clear interannual fluctuations in EEQ, whereas Xiamen and Fuzhou maintained relatively high EEQ levels in the early or middle stages but experienced fluctuations or declines in later years. Qingdao and Qinhuangdao also showed alternating increases and decreases, suggesting that ecological conditions did not improve linearly with urban development.

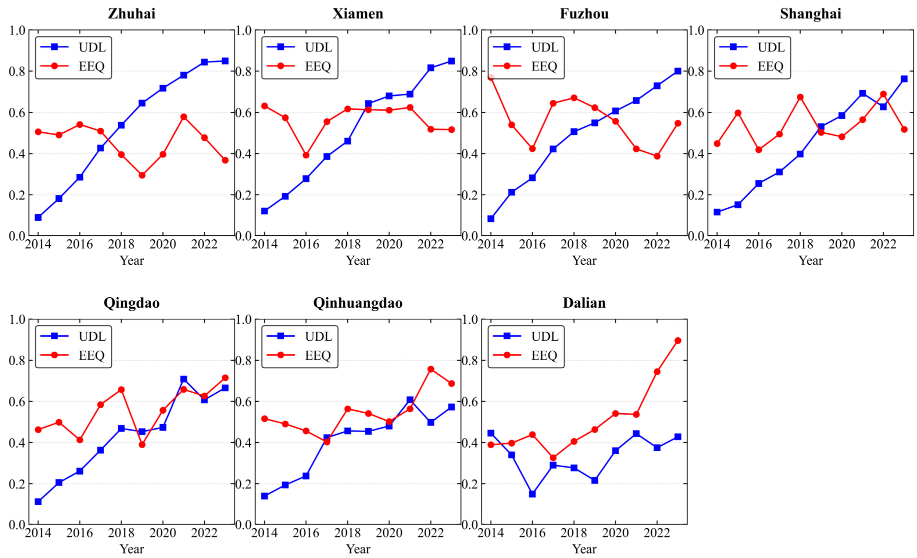

Figure 10. Evolution characteristics of UDL and EEQ.

Therefore, the relationship between UDL and EEQ should be interpreted as an asynchronous and city-specific evolutionary process rather than a simple convergence trend. In most cities, the continuous increase in UDL was accompanied by stable or fluctuating EEQ, indicating that urban development and ecological improvement were not fully synchronized. Dalian showed a distinct pattern, with relatively low and slightly fluctuating UDL but a marked increase in EEQ after 2020. Overall, the results suggest that coupling coordination depends not only on the growth of UDL but also on whether EEQ can be maintained or improved under increasing development pressure.

3.4. Coupling Coordination Analysis

Figure 11 illustrates the temporal evolution of CCD values for the seven coastal cities from 2014 to 2023. Overall, most cities exhibited increasing CCD values, indicating a gradual improvement in the coordination between urban development and the eco-environment. Zhuhai increased from 0.46 in 2014 to 0.75 in 2023, reaching the intermediate coordination level despite interannual fluctuations. Xiamen and Fuzhou showed relatively rapid improvements, increasing from 0.53 to 0.81 and from 0.50 to 0.81, respectively, and both reached the good coordination level by 2023.

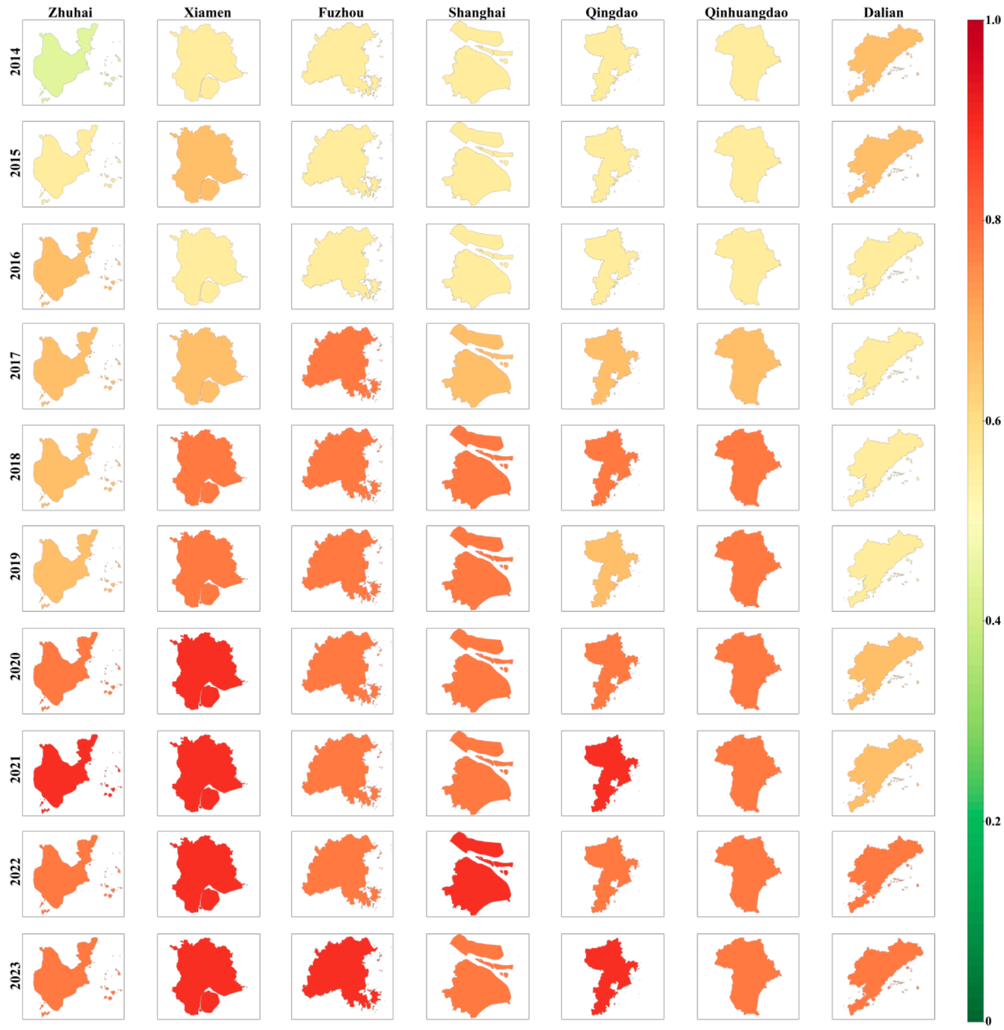

Figure 11. Temporal evolution of CCD.

Shanghai, Qingdao, and Qinhuangdao also showed overall upward trends, with CCD values increasing from 0.48 to 0.79, from 0.48 to 0.83, and from 0.52 to 0.79, respectively. Qingdao had the highest CCD value in 2023, indicating the most favorable coordination status among the seven cities. Dalian followed a different trajectory, declining from 0.65 in 2014 to 0.51 in 2016 before gradually recovering to 0.79 in 2023, close to the good coordination threshold. These results indicate that coupling coordination improved in most coastal cities, but the trajectories were not strictly linear and showed clear city-specific fluctuations.

Based on the CCD classification thresholds, values of 0.4–0.6, 0.6–0.8, and 0.8–1.0 were defined as Class 1, Class 2, and Class 3, respectively, to characterize the coordinated development levels of the seven coastal cities from 2014 to 2023 (Figure 12). Overall, the results show a gradual transition from Class 1 to Class 2, with only a few cities entering Class 3 in the later period.

Figure 12. CCD classification results during 2014–2023.

During 2014–2016, most cities were concentrated in Class 1, although Dalian reached Class 2 in 2014 and 2015. From 2017 to 2020, coordination levels generally improved, and most cities shifted to Class 2. However, this transition was not synchronous: Dalian remained in Class 1 until 2020, while Zhuhai and Qinhuangdao showed fluctuating changes. By 2021, all seven cities had entered Class 2, indicating a stage-wise improvement in overall coordination. During 2022–2023, several cities approached or exceeded the Class 3 threshold. Specifically, Fuzhou, Qingdao, and Qinhuangdao reached Class 3 in 2022, while Fuzhou and Shanghai remained in Class 3 in 2023. This indicates that the coordinated development of coastal cities had entered a stage of higher-level differentiation rather than a uniform transition to high coordination.

At the city level, Fuzhou showed the most stable improvement, increasing from 0.5042 in 2014 to 0.8137 in 2023. Shanghai also showed a generally upward trend and reached Class 3 in 2023. Xiamen maintained steady improvement and remained in the upper range of Class 2 in the later period. Qingdao increased markedly and entered Class 3 in 2022, but then declined slightly to Class 2 in 2023. Zhuhai and Qinhuangdao exhibited non-monotonic growth, whereas Dalian showed a recovery pattern, declining from Class 2 in the early stage to Class 1 during 2016–2020 before improving to Class 2 after 2021.

Spatially, southern coastal cities, including Xiamen, Fuzhou, Shanghai, and Zhuhai, generally maintained relatively higher or more stable coordination levels, whereas northern coastal cities, especially Qinhuangdao and Dalian, showed greater variability. Overall, the seven coastal cities gradually evolved from low coordination toward medium coordination, with a few cities reaching high coordination in the later years. Nevertheless, clear stage differences and pathway heterogeneity remained among cities.

3.5. Factor Importance Analysis

Figure 13 presents the Random Forest-based indicator importance analysis for the seven coastal cities. The upper-left, upper-right, and lower-left panels show the importance rankings of all indicators (X1–X22), UDL indicators (X1–X10), and EEQ indicators (X11–X22), respectively, while the lower-right panel shows the cumulative importance contribution curves. The dashed line indicates the 80% cumulative-importance threshold. The results show that CCD prediction was mainly associated with a limited number of high-contribution indicators: approximately 7–10 variables were needed to exceed this threshold when all indicators were considered, whereas the UDL and EEQ subsystems reached it with fewer variables. Random Forest importance represents predictive contribution rather than causal effects, so the top-ranked indicators are interpreted as associated explanatory variables.

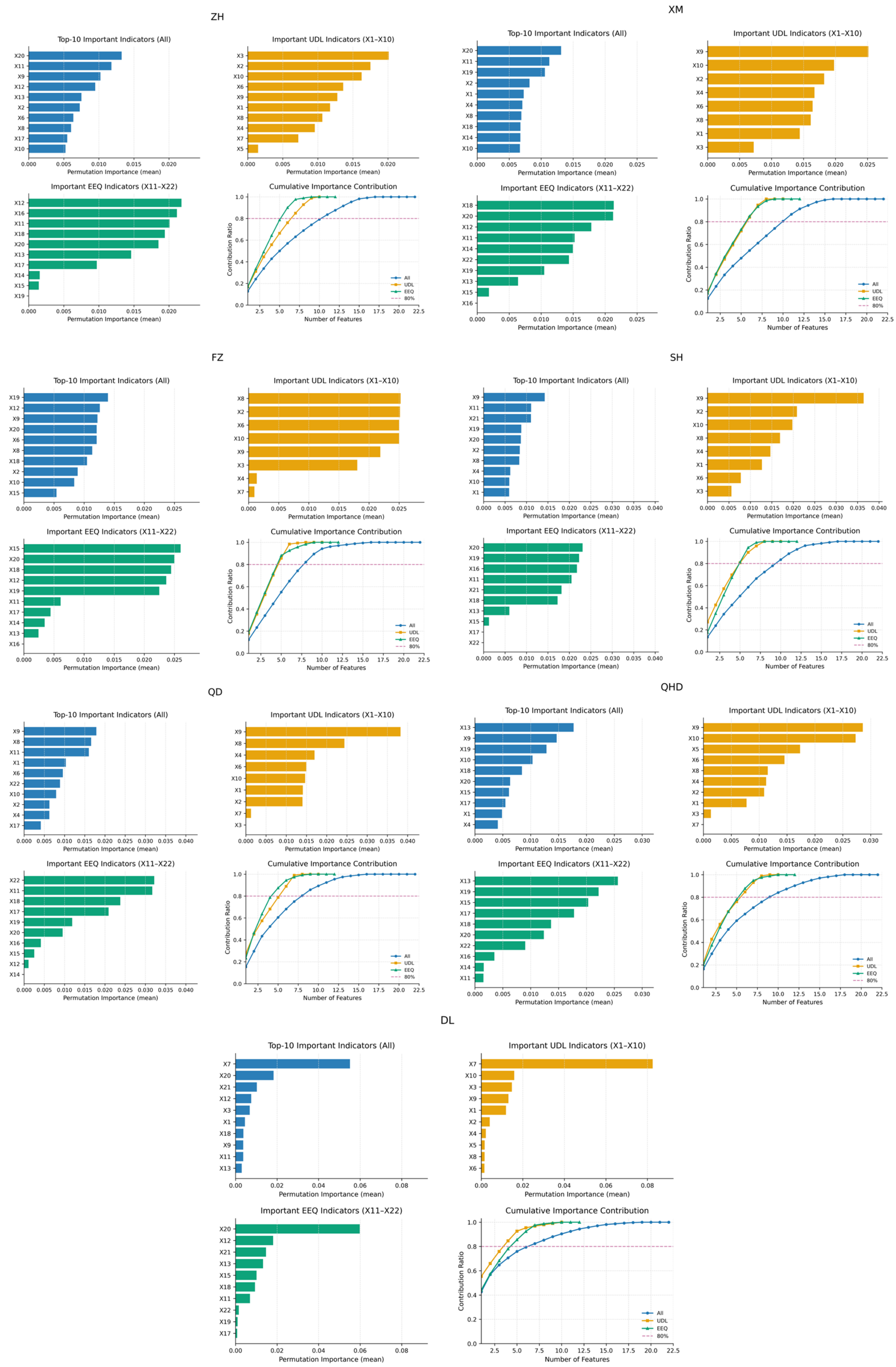

Figure 13. Random forest-based importance rankings of overall, UDL, and EEQ indicators.

Within the UDL subsystem, land-use-related indicators were prominent in most cities. Cultivated land ratio (X9) and construction land ratio (X10) ranked highly in several cities, while population size (X2), population density (X3), fixed asset investment (X6), the proportion of secondary and tertiary industries (X8), and per capita retail sales of consumer goods (X7) also showed high importance in specific cities. These results suggest that land-use structure, population agglomeration, and economic activity were closely associated with UDL-related variation in CCD prediction.

For the EEQ subsystem, ecological condition, land-cover composition, and pollution-related indicators contributed substantially to CCD prediction. Biological richness index (X20), vegetation coverage index (X19), forest land proportion (X12), grassland proportion (X11), and bare land proportion (X13) frequently appeared among the high-importance variables. Industrial wastewater discharge (X17) and sulfur dioxide emissions (X18) were also important in several cities, indicating the contribution of environmental pressure variables.

When all indicators were considered simultaneously, the Random Forest results showed distinct city-specific patterns. As summarized in Table 5, the top three indicators were X20, X11, and X9 in Zhuhai; X20, X11, and X19 in Xiamen; X19, X12, and X9 in Fuzhou; X9, X11, and X21 in Shanghai; X9, X8, and X11 in Qingdao; X13, X9, and X19 in Qinhuangdao; and X7, X20, and X21 in Dalian. These differences indicate spatial heterogeneity in the indicators associated with CCD prediction and may reflect variations in development stage, land-use structure, ecological conditions, and environmental pressure.

Table 5. Top three overall indicators associated with CCD prediction in each city.

City	Top Indicator 1	Top Indicator 2	Top Indicator 3
Zhuhai (ZH)	X20	X11	X9
Xiamen (XM)	X20	X11	X19
Fuzhou (FZ)	X19	X12	X9
Shanghai (SH)	X9	X11	X21
Qingdao (QD)	X9	X8	X11
Qinhuangdao (QHD)	X13	X9	X19
Dalian (DL)	X7	X20	X21

4. Discussion

4.1. Stage-Wise Evolution of UDL, EEQ, and CCD

The results show that the CCD values of the seven coastal cities generally increased from 2014 to 2023, suggesting that the relationship between urban development and the eco-environment shifted toward improved coordination. This finding is broadly consistent with previous studies showing that coupling coordination between urbanization and the eco-environment tends to improve over time in rapidly urbanizing regions, such as the Cheng-Yu Urban Agglomeration and the Chengdu–Chongqing Urban Agglomeration [36,37]. Similar stage-wise or nonlinear coordination patterns have also been reported for Shanghai and the Beijing–Tianjin–Hebei region [38,39].

However, the improvement observed in this study should not be interpreted as a simple linear outcome of economic growth. The temporal trajectories of UDL, EEQ, and CCD indicate an asynchronous and city-specific evolution process. In most cities, UDL increased steadily, whereas EEQ showed more complex fluctuations, suggesting that urban development and ecological improvement were not fully synchronized. The transition from lower to moderate coordination may be associated with improvements in urban development, infrastructure construction, and environmental management capacity. In contrast, the transition from moderate to higher coordination appears to depend more on integrated improvements in land-use efficiency, industrial upgrading, ecological restoration, and governance continuity.

Compared with previous CCD studies focusing on general urban agglomerations or inland regions, this study highlights the particularity of coastal cities. These cities are characterized by intensive land development, population agglomeration, port-related economic activities, and strong ecological constraints. Therefore, their coordinated development depends not only on improved urban development levels but also on whether eco-environmental quality can be maintained or enhanced under increasing development pressure.

4.2. Spatial Heterogeneity and Differentiated Development Pathways

Although the sampled cities showed an overall improvement in CCD, their development pathways were not uniform. The results reveal clear spatial heterogeneity among coastal cities, indicating that urban development–eco-environment coordination is highly context-dependent. Previous studies have also reported significant spatial heterogeneity in urbanization–eco-environment coordination, including east–west or southeast–northwest differences in Chinese urban agglomerations and provincial capital cities [36,40]. This study further shows that, even among coastal cities with similar geographical attributes, coordination pathways can differ markedly due to variations in development stage, industrial structure, land-use intensity, ecological endowment, and governance priorities.

For highly urbanized cities such as Shanghai, maintaining coordination under high development intensity may depend more on land-use efficiency, compact spatial organization, and continuous environmental governance. This is consistent with previous research on Shanghai, which emphasized that urbanization pressure and ecological responses jointly shape coupling coordination trajectories [38]. For port–industrial or manufacturing-oriented cities, coordinated improvement may be more closely associated with industrial restructuring, pollution reduction, and wastewater treatment capacity. For tourism-oriented and ecologically livable coastal cities, maintaining vegetation conditions, habitat quality, and ecological resilience is important for sustaining relatively high coordination levels, which is consistent with studies emphasizing the need to balance tourism urbanization benefits with ecological impacts [41].

Therefore, coastal cities should not adopt a uniform development strategy. Instead, type-oriented and region-specific pathways are more appropriate for improving coordination. Highly urbanized cities should emphasize land-use efficiency and spatial optimization, port–industrial cities should focus on industrial transformation and pollution control, and ecologically livable or tourism-oriented cities should prioritize ecological conservation and habitat quality improvement.

4.3. Variable Importance Patterns and Policy Implications

The random forest results indicate that the variable importance structure associated with CCD prediction is highly concentrated, with the top 7–10 indicators explaining more than 80% of the coordination-related information in most cities. This suggests that CCD prediction is mainly associated with a limited number of high-contribution indicators, rather than being evenly explained by all variables. This finding is consistent with previous studies showing that different indicators contribute unevenly to urbanization–eco-environment coupling systems and that land use, population agglomeration, economic activity, pollution control, and ecological responses often play important but region-specific roles [38,42,43].

It should be emphasized that RF importance reflects the relative contribution of variables to model prediction rather than direct causal effects. Therefore, these indicators should be interpreted as important explanatory or associated variables related to CCD evolution, rather than as strict causal drivers. In this study, the UDL subsystem is strongly associated with land-use structure and population agglomeration, whereas the EEQ subsystem is closely related to pollution pressure and ecosystem conditions. These results are generally consistent with previous findings that rapid urbanization and industrial expansion can intensify land-use change and eco-environmental stress, while ecological restoration, pollution control, and green infrastructure construction can contribute to improved coordination [37,41,44].

From a policy perspective, the heterogeneous importance patterns are broadly consistent with differences in development strategies and environmental governance practices among coastal cities. For highly urbanized cities, improving land-use efficiency and optimizing urban spatial structure are particularly important; practical measures may include compact redevelopment, brownfield reuse, mixed land-use planning, and the expansion of urban green–blue infrastructure. For port–industrial cities, reducing industrial emissions and improving wastewater treatment capacity remain key policy priorities, which can be supported by stricter industrial discharge monitoring, cleaner production, and upgrades to wastewater treatment facilities. For tourism-oriented and ecologically livable coastal cities, maintaining vegetation conditions, habitat quality, and ecological resilience is essential for sustaining higher coordination levels; therefore, habitat conservation, ecological corridor construction, and coastal wetland restoration should be emphasized. Accordingly, the RF results should be understood as evidence of variable importance and policy-relevant associations rather than as direct causal proof of driving mechanisms.

4.4. Applicability, Limitations, and Future Work

The applicability of the conclusions should be understood in relation to the characteristics of the selected coastal cities. The findings are most relevant to coastal cities characterized by intensive land development, population agglomeration, port-related economic activities, and ecological pressure, particularly when long-term statistical and remote sensing data are available. The proposed framework, which integrates an ecologically enhanced indicator system, adaptive weighting, CCD measurement, and variable importance analysis, can be extended to other coastal urban regions with similar data availability.

However, the broader generalization of specific results should be treated with caution. Previous studies have shown that the coordination relationship between urbanization and the eco-environment varies across regions due to differences in ecological background, urbanization stage, industrial structure, and governance systems [39,40,43]. Therefore, when applying this framework to other regions or countries, the indicator system, weighting strategy, CCD thresholds, city classification criteria, and interpretation of high-importance variables should be adjusted according to local conditions.

In addition, the final EEQ construction involves the integration of heterogeneous ecological dimensions. Although the equal-weight strategy provides a transparent baseline for integrating the environmental-factor composite value, NDVI, and DHI, different fusion weights may still affect the magnitude of the EEQ and CCD values to some extent. Future studies could further introduce sensitivity analysis or data-driven fusion strategies to examine the robustness of EEQ construction under different weighting scenarios. Moreover, finer-resolution spatial analysis, pixel-level ecological change detection, scenario simulation, and causal inference methods could be incorporated to better distinguish local ecological changes, policy effects, and long-term coordination mechanisms.

5. Conclusions

Based on the above analysis, the main conclusions of this study are summarized from the perspectives of framework construction, temporal evolution, associated factor identification, and differentiated governance.

1. This study constructed an integrated analytical framework combining an ecologically enhanced indicator system, EWM–MLP adaptive weighting, CCD measurement, and RF-based variable importance analysis. The framework characterizes coupling coordination between urban development and eco-environmental systems in coastal cities from the perspectives of temporal variation, nonlinear adjustment, and urban heterogeneity. The EWM–MLP strategy refined the entropy-derived weights while maintaining the overall stability of CCD classification, providing a useful approach for coastal urban sustainability assessment.
2. From 2014 to 2023, the CCD values of the seven coastal cities generally increased, indicating that the relationship between urban development and the eco-environment shifted toward improved coordination. However, the evolution was not strictly linear. UDL generally increased in most cities, whereas EEQ showed more complex and fluctuating trajectories, indicating that urban development and ecological improvement were not fully synchronized. The transition from lower to moderate coordination was relatively rapid in some cities, whereas further improvement toward higher coordination depended more on the simultaneous enhancement of development quality, ecological resilience, land-use efficiency, and governance continuity.
3. The RF-based variable importance results indicate that the predictive contribution to CCD was mainly concentrated in a limited number of high-contribution indicators. For all indicators combined, approximately 7–10 top-ranked variables were generally required to exceed 80% of the total importance, while the UDL and EEQ subsystems reached the threshold with fewer indicators. The UDL subsystem was mainly associated with land-use structure, population agglomeration, and economic activity, whereas the EEQ subsystem was related to ecological conditions, land-cover composition, and environmental pressure. RF importance should be interpreted as the relative contribution of variables to prediction rather than as evidence of direct causal mechanisms.
4. The coordination pathways and high-contribution indicators differed markedly among coastal cities, indicating that type-specific governance is more practical than a uniform governance approach. Highly urbanized cities should focus on land-use efficiency and spatial optimization; port–industrial cities should strengthen industrial transformation and pollution control; and tourism-oriented or ecologically livable cities should prioritize vegetation conditions, habitat quality, and ecological resilience. Future studies can further improve the robustness of urban ecological assessment and the interpretation of coordination mechanisms by incorporating longer time series, larger samples, higher-resolution data, sensitivity analysis, scenario simulation, and causal inference methods.

Author Contributions: Conceptualization, Q.Z., Y.G. and J.Y.; methodology, Q.Z. and Z.Y.; software, Q.Z. and H.X.; validation, Q.Z., Y.G. and J.Y.; formal analysis, Q.Z. and H.X.; investigation, Q.Z. and H.X.; resources, Y.G.; data curation, Q.Z.; writing—original draft preparation, Q.Z.; writing—review and editing, Q.Z. and H.X.; visualization, Q.Z. and H.X.; supervision, Y.G. and J.Y.; project administration, Y.G.; funding acquisition, J.Y. and Z.Y. All authors have read and agreed to the published version of the manuscript.

Funding: This research was funded by the Science and Technology Projects of Social Development in Zhuhai (2024 Annual), grant number 2420004000328.

Data Availability Statement: The Land Use Classification data were obtained from the Earth Resource Data Cloud (https://www.resdc.cn/DOI/DOI.aspx?DOIID=105 accessed on 15 December 2025), while the NDVI and Dynamic Habitat Index datasets were acquired from the National Earth System Science Data Center (https://www.geodata.cn/aboutus.html accessed on 19 December 2025). The other data used to support the findings of this study are available from the corresponding author upon request.

Conflicts of Interest: Author Jun Yan, Hongyin Xiang and Zhiyu Yan were employed by the company Zhuhai Aerospace Microchips Science & Technology. We declare that we have no financial and personal relationships with other people or organizations that could inappropriately influence our work, and there is no professional or other personal interest of any nature or kind regarding any product, service, and/or company that could be construed as influencing the position presented in, or the review of, the manuscript.

References

1. Oniang'o, R. Sustainable Development Goals. World Social Report. 2016. Available online: https://api.semanticscholar.org/CorpusID:131853122 (accessed on 15 November 2025).
2. Fang, Z.; Ding, T.; Chen, J.; Xue, S.; Zhou, Q.; Wang, Y.; Wang, Y.; Huang, Z.; Yang, S. Impacts of land use/land cover changes on ecosystem services in ecologically fragile regions. *Sci. Total Environ.* **2022**, *831*, 154967. [CrossRef]
3. Wang, Y.; Jiang, Y.; Li, W.; Dong, S.; Gao, C. Determinants of land use conflicts with the method of cross-wavelet analysis: Role of natural resources and human activities in spatial-temporal evolution. *J. Clean. Prod.* **2023**, *429*, 139498. [CrossRef]
4. Ling, Z.; Jiang, W.; Liao, C.; Li, Y.; Ling, Y.; Peng, K.; Deng, Y. Evaluation of Production–Living–Ecological Functions in Support of SDG Target 11.a: Case Study of the Guangxi Beibu Gulf Urban Agglomeration, China. *Diversity* **2022**, *14*, 469. [CrossRef]
5. Fang, J.; Xu, M.; Liu, B.; Chen, Z. An Evaluation of the Coordinated Development of Coastal Zone Systems: A Case Study of China's Yellow Sea Coast. *J. Mar. Sci. Eng.* **2022**, *10*, 919. [CrossRef]
6. Zhang, X.; Xu, Z. Functional Coupling Degree and Human Activity Intensity of Production–Living–Ecological Space in Underdeveloped Regions in China: Case Study of Guizhou Province. *Land* **2021**, *10*, 56. [CrossRef]
7. Hu, Y.; Chen, Y. Coupling of Urban Economic Development and Transportation System: An Urban Agglomeration Case. *Sustainability* **2022**, *14*, 3808. [CrossRef]
8. Cai, B.; Shao, Z.; Fang, S.; Huang, X. Quantifying Dynamic Coupling Coordination Degree of Human–Environmental Interactions during Urban–Rural Land Transitions of China. *Land* **2022**, *11*, 935. [CrossRef]
9. Wang, Y.; Liu, Y.; Zhou, G.; Ma, Z.; Sun, H.; Fu, H. Coordinated Relationship between Compactness and Land-Use Efficiency in Shrinking Cities: A Case Study of Northeast China. *Land* **2022**, *11*, 366. [CrossRef]
10. Liu, J.; Wang, H.; Hui, L.; Tang, B.; Zhang, L.; Jiao, L. Identifying the Coupling Coordination Relationship between Urbanization and Ecosystem Services Supply–Demand and Its Driving Forces: Case Study in Shaanxi Province, China. *Remote Sens.* **2024**, *16*, 2383. [CrossRef]
11. Ji, J.; Tang, Z.; Zhang, W.; Liu, W.; Jin, B.; Xi, X.; Wang, F.; Zhang, R.; Guo, B.; Xu, Z. Spatiotemporal and Multiscale Analysis of the Coupling Coordination Degree between Economic Development Equality and Eco-Environmental Quality in China from 2001 to 2020. *Remote Sens.* **2022**, *14*, 737. [CrossRef]
12. Gao, S.; Yang, L.; Jiao, H. Changes in and Patterns of the Tradeoffs and Synergies of Production-Living-Ecological Space: A Case Study of Longli County, Guizhou Province, China. *Sustainability* **2022**, *14*, 8910. [CrossRef]
13. Cheng, Z.; Zhang, Y.; Wang, L.; Wei, L.; Wu, X. An Analysis of Land-Use Conflict Potential Based on the Perspective of Production–Living–Ecological Function. *Sustainability* **2022**, *14*, 5936. [CrossRef]
14. Xu, N.; Chen, W.; Pan, S.; Liang, J.; Bian, J. Evolution Characteristics and Formation Mechanism of Production-Living-Ecological Space in China: Perspective of Main Function Zones. *Int. J. Environ. Res. Public Health* **2022**, *19*, 9910. [CrossRef]
15. Guo, Y.; Li, R.; Chen, J.; Chen, G.; Li, B.; Qiang, L.; Chang, J.; Wang, M. Driving Analysis of Spatiotemporal Change of Land Use in Production-Living-Ecology Space in Shendong Mining Area. *Int. J. Front. Eng. Technol.* **2020**, *2*, 302.
16. Zhang, P.; Zhang, J.; Yu, H.; Jiang, X.; Zhang, N. Research on the Identification, Network Construction, and Optimization of Ecological Spaces in Metropolitan Areas Based on the Concept of Production-Living-Ecological Space. *Sustainability* **2024**, *16*, 8228. [CrossRef]
17. Fu, Y.; Li, Q.; Li, J.; Zeng, K.; Wang, L.; Wang, Y. Multi-Scenario Simulation of the Production-Living-Ecological Spaces in Sichuan Province Based on the PLUS Model and Assessment of Its Ecological and Environmental Effects. *Sustainability* **2024**, *16*, 10322. [CrossRef]

18. Zhang, S.; Liu, S.; Zhong, Q.; Zhu, K.; Fu, H. Assessing Eco-Environmental Effects and Its Impacts Mechanisms in the Mountainous City: Insights from Ecological–Production–Living Spaces Using Machine Learning Models in Chongqing. *Land* **2024**, *13*, 1196. [CrossRef]
19. Li, W.; Tao, L.; Wen, C. Study on function evolution and coupling coordination degree of "Three Lives Space" in the upper reaches of Yangtze River in China. *Environ. Sci. Pollut. Res.* **2024**, *31*, 13026–13045. [CrossRef] [PubMed]
20. Qiao, W.; Hu, B.; Guo, Z.; Huang, X. Evaluating the sustainability of land use integrating SDGs and its driving factors: A case study of the Yangtze River Delta urban agglomeration, China. *Cities* **2023**, *143*, 104569. [CrossRef]
21. Wang, A.; Liao, X.; Tong, Z.; Du, W.; Zhang, J.; Liu, X.; Liu, M. Spatial-temporal dynamic evaluation of the ecosystem service value from the perspective of "production-living-ecological" spaces: A case study in Dongliao River Basin, China. *J. Clean. Prod.* **2022**, *333*, 130218. [CrossRef]
22. Tang, X.; Cai, L.; Du, P. Spatiotemporal Evolution and Driving Forces of Production-Living-Ecological Space in Arid Ecological Transition Zone Based on Functional and Structural Perspectives: A Case Study of the Hexi Corridor. *Sustainability* **2024**, *16*, 6698. [CrossRef]
23. Peng, Y.; Luan, Q.; Xiong, C. Evaluation of Spatial Functions and Scale Effects of "Production–Living–Ecological" Space in Hainan Island. *Land* **2023**, *12*, 1637. [CrossRef]
24. Han, S.; Wang, B.; Ao, Y.; Bahmani, H.; Chai, B. The coupling and coordination degree of urban resilience system: A case study of the Chengdu–Chongqing urban agglomeration. *Environ. Impact Assess. Rev.* **2023**, *101*, 107145. [CrossRef]
25. Tao, Y.; Wang, Q. Quantitative Recognition and Characteristic Analysis of Production-Living-Ecological Space Evolution for Five Resource-Based Cities: Zululand, Xuzhou, Lota, Surf Coast and Ruhr. *Remote Sens.* **2021**, *13*, 1563. [CrossRef]
26. Yang, Y.; Bao, W.; Liu, Y. Coupling coordination analysis of rural production-living-ecological space in the Beijing-Tianjin-Hebei region. *Ecol. Indic.* **2020**, *117*, 106512. [CrossRef]
27. De Toro, P.; Formato, E.; Fierro, N. Sustainability Assessments of Peri-Urban Areas: An Evaluation Model for the Territorialization of the Sustainable Development Goals. *Land* **2023**, *12*, 1415. [CrossRef]
28. Tang, Y.; Zhu, L.; Wang, X. Quantitative Analysis of the Evolution of Production–Living–Ecological Space in Traditional Villages: A Comparative Study of Rural Areas in Tibet. *Land* **2024**, *13*, 1889. [CrossRef]
29. Bendasiuk, O.; Shpylova, Y.; Neklyudova, T.; Sakharnatska, L. Socio-Ecological and Economic Paradigm of Sustainable Development of Rural Territories of Ukraine. Balanced Nature Using. 2022. Available online: https://api.semanticscholar.org/CorpusID:249946543 (accessed on 10 November 2025).
30. Tripathi, A.; Tiwari, R.K.; Tiwari, S.P. A deep learning multi-layer perceptron and remote sensing approach for soil health based crop yield estimation. *Int. J. Appl. Earth Obs. Geoinf.* **2022**, *113*, 102959. [CrossRef]
31. Wang, Z.; Ma, S.; Zhai, Y.; Huang, P.; Yang, X.; Cui, J.; Eridun, Q. Remote Sensing-Based Multilayer Perceptron Model for Grassland Above-Ground Biomass Estimation. *Appl. Sci.* **2025**, *15*, 6280. [CrossRef]
32. Jiang, W.; He, G.; Long, T.; Ni, Y.; Liu, H.; Peng, Y.; Lv, K.; Wang, G. Multilayer perceptron neural network for surface water extraction in Landsat 8 OLI satellite images. *Remote Sens.* **2018**, *10*, 755. [CrossRef]
33. Al-Dousari, A.E.; Mishra, A.; Singh, S. Land use land cover change detection and urban sprawl prediction for Kuwait metropolitan region, using multi-layer perceptron neural networks (MLPNN). *Egypt. J. Remote Sens. Space Sci.* **2023**, *26*, 381–392. [CrossRef]
34. He, X.; Chen, Y. Modifications of the multi-layer perceptron for hyperspectral image classification. *Remote Sens.* **2021**, *13*, 3547. [CrossRef]
35. *HJ/T 192-2006*; Technical Criterion for Eco-Environmental Status Evaluation. China Environmental Science Press: Beijing, China, 2006.
36. Yang, L.; Zhang, X.; Pan, J.; Yang, Y. Coupling coordination and interaction between urbanization and eco-environment in Cheng-Yu urban agglomeration, China. *Chin. J. Appl. Ecol.* **2021**, *32*, 993–1004. [CrossRef]
37. Lei, X.; Liu, H.; Li, S.; Luo, Q.; Cheng, S.; Hu, G.; Wang, X.; Bai, W. Coupling coordination analysis of urbanization and ecological environment in Chengdu-Chongqing urban agglomeration. *Ecol. Indic.* **2024**, *161*, 111969. [CrossRef]
38. He, J.; Wang, S.; Liu, Y.; Ma, H.; Liu, Q. Examining the relationship between urbanization and the eco-environment using a coupling analysis: Case study of Shanghai, China. *Ecol. Indic.* **2017**, *77*, 185–193. [CrossRef]
39. Wang, S.; Ma, H.; Zhao, Y. Exploring the relationship between urbanization and the eco-environment—A case study of Beijing–Tianjin–Hebei region. *Ecol. Indic.* **2014**, *45*, 171–183. [CrossRef]
40. Fan, Y.; Fang, C.; Zhang, Q. Coupling coordinated development between social economy and ecological environment in Chinese provincial capital cities-assessment and policy implications. *J. Clean. Prod.* **2019**, *229*, 289–298. [CrossRef]
41. Ma, M.; Tang, J. Interactive coercive relationship and spatio-temporal coupling coordination degree between tourism urbanization and eco-environment: A case study in Western China. *Ecol. Indic.* **2022**, *142*, 109149. [CrossRef]
42. Li, W.; Yi, P. Assessment of city sustainability—Coupling coordinated development among economy, society and environment. *J. Clean. Prod.* **2020**, *256*, 120453. [CrossRef]

43. Cai, J.; Li, X.; Liu, L.; Chen, Y.; Wang, X.; Lu, S. Coupling and coordinated development of new urbanization and agro-ecological environment in China. *Sci. Total Environ.* **2021**, *776*, 145837. [CrossRef]
44. Kyule, B.M.; Wang, X. Quantifying the link between industrialization, urbanization, and economic growth over Kenya. *Front. Archit. Res.* **2024**, *13*, 799–808. [CrossRef]